Journal of *Marine Science and Engineering*

MDPI

Article

The Lateral Behavior of Large-Diameter Monopiles for Offshore Wind Turbines Based on the p-y Curve and Solid FEM Methods

Tao Li [1,†], Xinran Yu [2,†], Ben He [3,*] and Song Dai [2,*]

[1] CSSC Haizhuang Windpower Co., Ltd., Chongqing 401147, China; litaoli12@163.com
[2] School of Civil Engineering, Shandong University, Jinan 250061, China; 202215034@mail.sdu.edu.cn
[3] Power China Huadong Engineering Corporation Ltd. (HDEC), Key Laboratory of Far Shore Wind Power Technology of Zhejiang Province, Hangzhou 311122, China
* Correspondence: he_b2@ecidi.com (B.H.); dais1027@sdu.edu.cn (S.D.)
† These authors contributed equally to this work.

Abstract: With the rapid increase in offshore wind turbines in China, monopiles with diameters exceeding 2 m are widely used. As these piles are subjected to lateral loads caused by wind, waves, and currents, the designs of the pile foundations supporting the offshore wind turbines are significantly influenced by their lateral behaviors. For this reason, field tests of the largest monopile on the sea and additional analysis based on the solid finite element method (FEM) and p-y curves are carried out to reveal the response of monopiles subjected to lateral loads and to figure out key technical issues related to the design process. The results revealed that the p-y curves proposed by the API code for clay showed a much "softer" response, which resulted in the conservative design of the piles. The solid FEM relied heavily on the choosing of the parameters used. At relatively small deflections, the solid FEM presented reasonable results as compared with the tests which were, however, supposed to overestimate the ultimate capacity of the piles. The results also indicated the importance of the influence of the pile–soil gap and the application of parameter analysis to achieve relatively conservative results, if the solid FEM is adopted in the design.

Keywords: field test; monopile; lateral load; p-y curve; solid finite element method

Citation: Li, T.; Yu, X.; He, B.; Dai, S. The Lateral Behavior of Large-Diameter Monopiles for Offshore Wind Turbines Based on the p-y Curve and Solid FEM Methods. *J. Mar. Sci. Eng.* **2023**, *11*, 2354. https://doi.org/10.3390/jmse11122354

Academic Editor: Erkan Oterkus

Received: 10 November 2023
Revised: 1 December 2023
Accepted: 4 December 2023
Published: 13 December 2023

1. Introduction

Due to the increasingly serious energy shortage and environmental pollution, the global energy structure has progressively converted from fossil fuels to low-carbon energy since the beginning of the 21st century and entered the era of low-carbon energy dominated by clean and renewable energy [1–4]. The strategic target of "carbon peak and carbon neutral" was solemnly declared by China in 2020. The vigorous development of clean and renewable energy has become an important way to achieve the strategic goal of "carbon peak and carbon neutral" and to ensure the coordinated development of the economy and environment. Among many renewable energy sources, offshore wind power has become the focus of global new energy development due to its unique advantages, i.e., abundant resources, stable wind speed, soil saving, and easy large-scale development [5–8].

Offshore wind power first originated in Europe, while offshore wind power in China started relatively late. However, under the guidance of some relevant policies, offshore wind power in China has developed rapidly, and the cumulative installed capacity has been ranked first, becoming the most important market in the world. With the rise and rapid development of offshore wind power in China, large-diameter steel pipe monopiles with diameters of 2–6 m have been widely used [9]. Due to the coupling effect of horizontal loadings, i.e., wind loading, including the operational loading of the wind turbine, wave loading, and current loading, of which the relevant data can be used to evaluate the potential of wind power generation in wind farms, actual interaction between the wind turbine and the site is realized [10,11]. Therefore, the horizontal bearing characteristics

of the pile foundation are the controlling factor in the design of large-diameter steel pipe monopile foundations for offshore wind turbines [12,13].

At present, the p-y curve method [14,15] and the solid FEM [16] are usually used in the design of large-diameter monopile foundations for offshore wind turbines. Cheng et al. [17] used the finite element method to systematically investigate the impact of different cyclic loading patterns on the lateral responses of large-diameter monopiles. Kato et al. [18] made up for the gap in the ability to accurately estimate the post-storm frequency change in offshore wind turbines due to soil stiffness degradation through the finite element method. However, there are certain problems and limitations for the p-y curve method and solid FEM in the design of monopile foundations for offshore wind turbines. For the p-y curve method, the p-y curve recommended by common specifications is established by the test results of a flexible pile with a small diameter, i.e., the API specification [19], NDV specification [20], and the code for pile foundations of harbor engineering [21]. Mu et al. [22] modified the ultimate resistance of sand in the API p-y model to consider the additional friction of the vertical load on the soil wedge. Lu et al. [23] proposed a new p-y curve model for vertical–horizontal loading conditions combined with the finite element model and summarized the reference values suitable for engineering applications. Moreover, the "size effect" caused by the increase in the pile diameter and the relative stiffness of the pile and soil causes the transformation of the displacement field of the soil around the pile and failure mode, which results in the inaccurate reflection of traditional calculation methods on real deformation characteristics and the ultimate bearing capacity of the pile foundation in the design process of large-diameter monopile foundations [24,25]. Compared with the p-y curve method, the continuity of the soil and the transformation of the displacement field failure mode caused by the "size effect" of large-diameter piles are taken into consideration in the solid FEM, however, the accuracy of the solid FEM depends on the selection of the soil constitutive model and corresponding parameters. In addition, few soil parameters can be obtained in actual offshore wind power projects, which makes the relatively advanced soil constitutive model different when directly applied to offshore wind turbine foundation design. The PISA method selects a four-spring (SSI) model, which not only considers the distributed lateral load spring but also additional the soil spring, which has an important effect on the lateral response of the piles. The single pile presents a higher safety margin, and the optimum pile foundation design can finally be obtained.

Aiming at the defects and problems existing in the design of large-diameter steel pipe monopile foundations for offshore wind turbines, the offshore full-scale in situ testing of large-diameter piles is carried out in the sea area of Jiangsu Province, China. The diameter of the testing pile is 2.8 m, which is the largest diameter of an offshore in situ testing pile recorded in China, and the in situ loading characteristics of the large-diameter monopile foundation are revealed. Based on the field test results, the applicability and reliability of the p-y curve method and solid FEM are evaluated in the design of large-diameter monopile foundations, which provide a corresponding reference for the current design of monopile foundations for offshore wind turbines.

2. Offshore Full-Scale In Situ Test of Pile

2.1. Testing Pile Arrangement and Soil Seabed Parameters

The full-scale in situ testing pile is located near the offshore sea of Jiangsu Province, China, and the layout of the offshore testing pile and the reaction pile is shown in Figure 1. The diameter of the testing pile (S1 and S2) is 2.8 m, and the length of the embedded mud surface is 72.5 m, while the loading point for the horizontal load is 20.3 m above the mud surface. As shown in Figure 1a, the distance between the two testing piles is 11.2 m, and a drilling position and point location of a cone penetration test (CPT) are arranged between two testing piles to acquire property parameters of the soil seabed near testing piles. Moreover, the site operation of offshore testing piles is illustrated in Figure 1b.

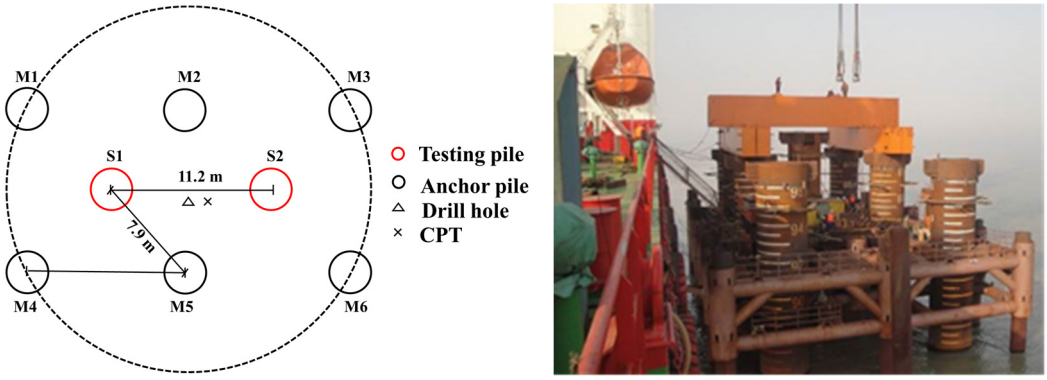

Figure 1. Layout of in situ test. (**a**) Arrangement schematic diagram of offshore testing piles. (**b**) Site operation of offshore testing pile.

Results of the CPT and undrained shear strength of soil (s_u) are presented in Figure 2. The shallow soil (0–16 m below soil surface) is mainly mucky silty clay, and the undrained shear strength of the mucky silty clay can be obtained by the following Formula (1) based on the resistance of the cone tip (q_c). σ_{vo} is the total overburden stress of soil, and N_k is the strength parameter. In addition, the soil specimens obtained from boreholes are used for laboratory triaxial tests. According to the UU test results of drilled soil samples, when the strength parameter N_k is set to 30, the undrained shear strength of soil (s_u) from the CPT is most consistent with UU test results. Therefore, for the soil site in the offshore full-scale in situ test of the pile, the N_k is uniformly 30, which is close to the property parameter of marine soil recommended by Lu Fengci [26].

$$s_u = \frac{q_c - \sigma_{vo}}{N_k} \tag{1}$$

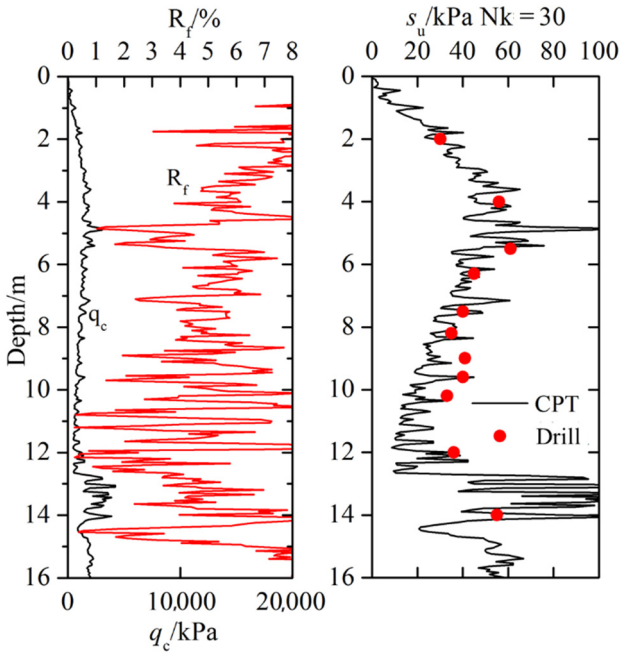

Figure 2. Results of CPT and undrained shear strength of soil.

The soil seabed from 16 m below the mud surface to the pile bottom is sand, and the average effective internal friction angle of the sand seabed (φ) is 32°. Since the lateral loading behavior of the large-diameter pile is determined by the shallow soil within 5–10 D, therefore, mechanical properties and testing results of deep soil are not discussed in detail herein.

2.2. Testing Instrument Arrangement and Loading Method

In order to obtain the bending moment of the pile section and calculate the horizontal displacement of the pile body, a copper strip fiber-optic sensing cable is arranged along the depth direction of the pile body (from the loading point to 22 m below the mud surface), as shown in Figure 3. Firstly, the optical cable is directly connected to the polished steel pipe pile in the form of welding, and the fiber-optic sensing cable is covered with epoxy resin adhesive, which is smeared along the laid line of the sensing cable to make it firmly attach to the grinding pile surface. Then, after the optical cable is installed, gold foil paper and asbestos cloth are laid on its surface for protection, and the optical cable is covered by an angle iron to prevent the optical fiber being damaged in the piling process. The bending moment and deflection of the pile body can be effectively calculated based on the measurement data from the optical cable.

The slow maintenance loading method by graded loading is adopted for horizontal loading in offshore full-scale in situ tests of the pile [27]. The testing reaction device is the 1000 kN class reaction beam system, and the testing reaction force is provided by four anchor piles. The loading system consists of three parts, i.e., a 600 kN horizontal type oil jack, 70 MPa ultra-high pressure oil circuit, and oil pump. Moreover, the testing data are automatically measured by the RS-JYC static test system, and the horizontal loading in the loading and unloading process is controlled by a 1000 kN class BHR-4 pressure sensor. The horizontal load is transmitted to the testing pile body through a spherical hinge on the top of a horizontal type oil jack. Before the horizontal loading is loaded, the load-carrying part of the pile head is strengthened to avoid local yield failure caused by the stress concentration. The maximum loading of the S1 testing pile is 425 kN, while that of the S2 testing pile is 500 kN.

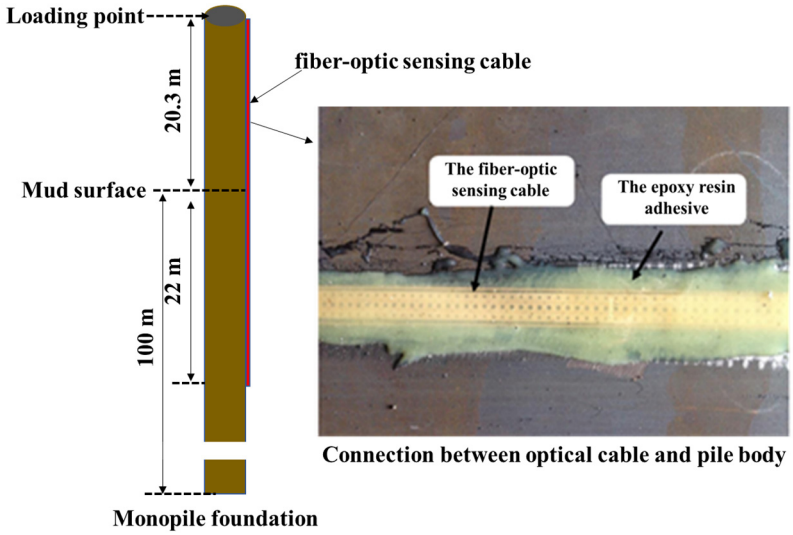

Figure 3. Testing pile schematic and connection between optical cable and pile body.

2.3. Testing Result and Analysis

The horizontal loading–deflection behaviors of testing piles S1 and S2 at the horizontal loaded location and mud surface are illustrated in Figure 4. Within the range of the applied loading (less than 500 kN), the horizontal loading–deflection behavior of the testing pile at the horizontal loaded location and mud surface presented a linear relationship. However,

there are some differences in the lateral loaded behavior of testing piles S1 and S2, for instance, the stiffness of the pile head of testing pile S1 is less than that of S2, and the residual displacement of the pile head of testing pile S1 is more than that of S2. The main reason for the above phenomenon may be the property difference of the soil seabed near testing piles S1 and S2. In detail, the distance between testing piles S1 and S2 is 11.2 m, and the property difference will be revealed by the p-y curve in Section 3.1.

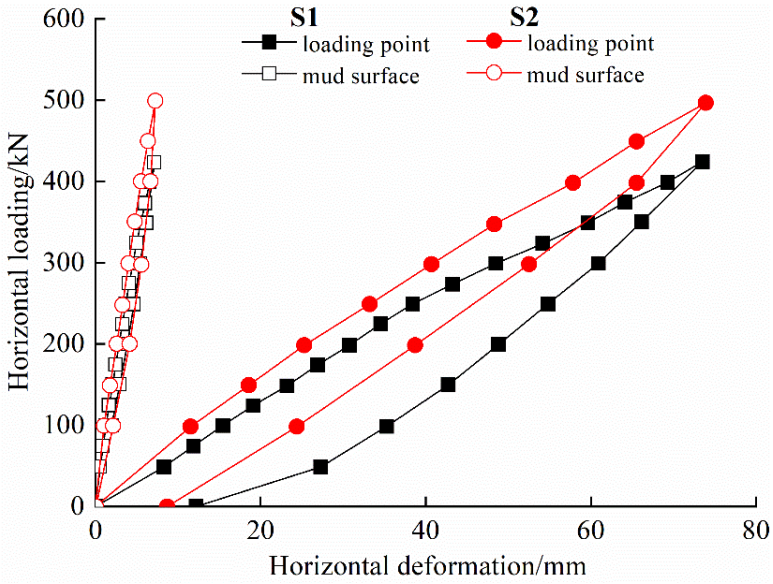

Figure 4. Horizontal loading–deflection behavior of pile.

The bending moment and displacement of testing pile S2 under various horizontal loadings are shown in Figure 5, and it is obvious that the testing pile shows a typical flexible response under horizontal loading. The influence of horizontal loading on the bending moment and deformation of the testing pile is up to 16 m below the mud surface (5.7 *D*, *D* is pile diameter), and the pile outside the 5.7 *D* range is hardly affected by the upper horizontal loading. The maximum bending moment and the first inverse bending moment point of the testing pile appear 2 m (0.71 *D*) and 7.5 m (2.7 *D*) below the mud surface, respectively. With the increase in horizontal loading, the maximum bending moment and the first inverse bending moment point of the testing pile gradually move down and tend to be stable (1.1 *D* and 4.5 *D* below the mud surface, respectively).

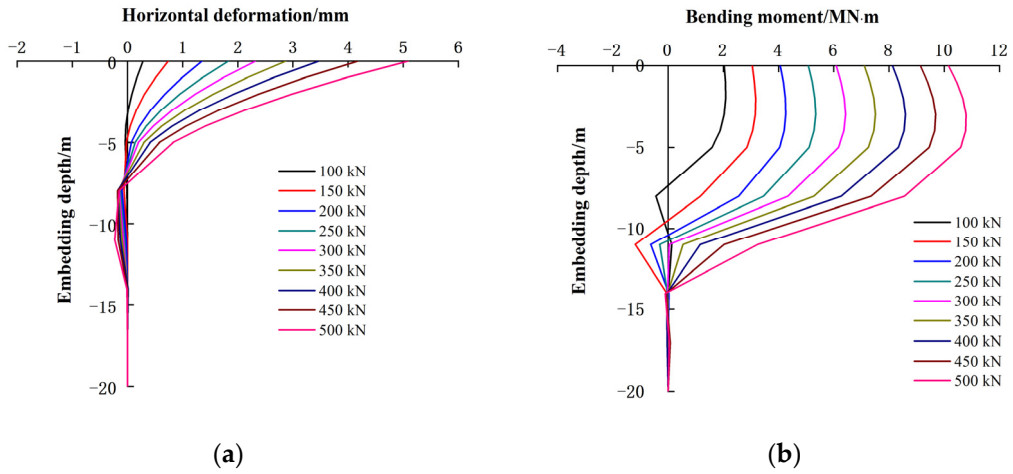

Figure 5. Distribution of pile deformations and bending moments subjected to different lateral loadings. (**a**) Horizontal deformation of pile. (**b**) Section bending moment of pile.

In order to further analyze field-testing results, based on field-testing data the field test process is restored and key technical problems of large-diameter monopile foundation design of offshore wind turbines are discussed deeply by the combined method of the p-y curve method and the solid finite element method.

3. Testing Pile Analysis Based on the P-Y Curve and Solid Finite Element Method

3.1. The P-Y Curve Method

The principle of the p-y curve method is to discretize the soil to a discontinuous spring along the depth direction of the pile, and the horizontal interaction between pile and soil can be described by the load–displacement response of the spring. Due to the simple principle of the p-y curve method, it can comprehensively consider the nonlinearity of soil, the stiffness of the pile, and the external load characteristics, and it is suitable for large deformation analysis, making the p-y curve method the most widely used design method for the monopile foundations of offshore wind turbines.

The p-y curve recommended by the API specification is adopted in the study [14,28], and the process of testing the pile is simulated in ABAQUS (v6.14) finite element software [29]. The pile body in the calculation simulation is adopted as a beam element, the beam mesh is set to 1 m, and the size data of the pile section are completely consistent with the testing pile in the offshore in situ test, as shown in Figure 6. The soil is equivalent to discontinuous nonlinear springs, and springs are set at a 1 m interval scale. It can be found from the field test data that the influence depth of horizontal loading is only 16 m, so the pile is truncated at 30 m below the mud surface in the study to reduce unnecessary modeling and iterative calculation time. The horizontal loading is imposed 20.3 m above the mud surface in the form of concentrated loading, which is consistent with the loading height of the testing pile in the offshore in situ test.

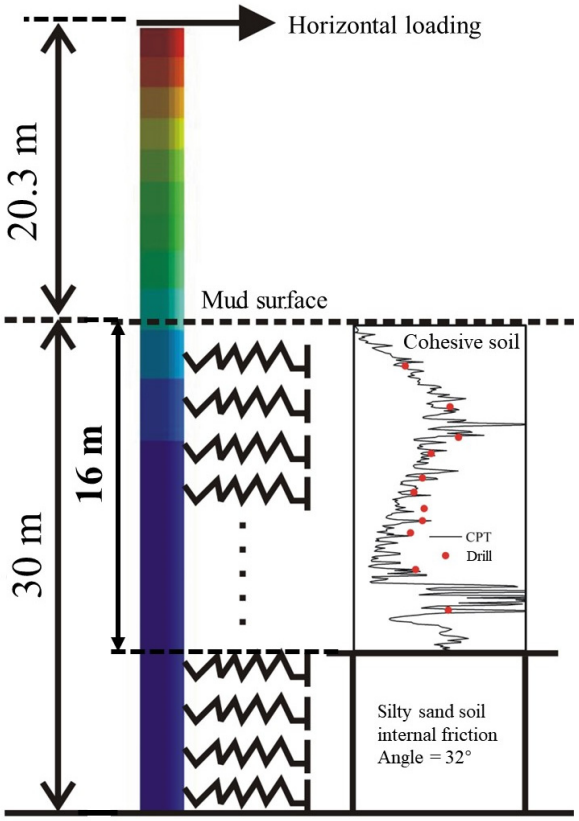

Figure 6. Schematic of model of p-y method.

3.2. The Solid Finite Element Method

The three-dimensional finite element simulation is also carried out in the ABAQUS (v6.14) finite element software, and the numerical model of pile–soil interaction is consistent with the testing pile in field tests. The 3D numerical model of pile–soil interaction and finite element mesh is shown in Figure 7, and the 8-node 6-face reduction integral element (C3D8R) is adopted to describe the pile and soil. The mesh density in the model is doubled, and each layer is divided into 48 meshes with 49 layers, a total of 2352 meshes. Th influence on the calculation result is less than 1%, which proves the reliability of the model mesh in this study. To avoid the influence of boundary conditions, the soil diameter is set as 28 m (10 D), and the height is 100 m. In addition, the bottom boundary of the soil model is completely fixed, and the lateral boundary is restricted in the axial and tangential displacement. The diameter and embedded length of the pile model are consistent with the testing pile, which are 2.8 m and 72.5 m, respectively. Coulomb friction interaction is used to describe the contact relation between the pile surfaces and soil surfaces, pile surfaces are set as the master surfaces, and the soil surfaces are set as the slave surfaces. Based on the suggestion recommended by Wang and Chen [30], the friction coefficient of interaction surfaces between the pile and soil is in the range of 0.2 and 0.4. Therefore, the friction coefficient of Coulomb friction interaction in the solid calculation simulation is set as 0.3, and the parametric analysis of the friction coefficient will be performed below.

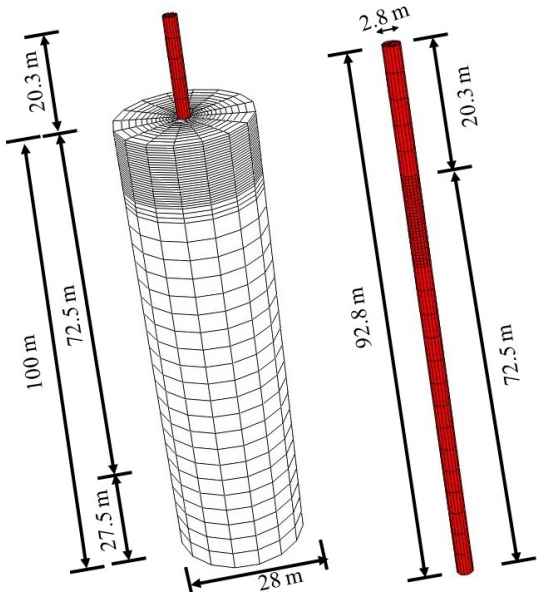

Figure 7. Solid finite element model of pile–soil interaction.

The ideal elastic–plastic constitutive model combined with the Moore–Coulomb failure criterion is adopted as the constitutive model of soil in the calculation simulation. For the cohesive soil in a shallow layer, considering that the soil is undrained during loading, two constitutive parameters are defined, i.e., the undrained shear strength s_u and the undrained Young's modulus E_u. The undrained shear strength can be directly obtained from CPT data (Figure 2). Assuming that the ratio of the undrained Young's modulus and undrained shear strength (E_u/s_u) is constant, the ratio E_u/s_u of soil is determined to be 400 according to the recommendation by Ou [31], and the corresponding sensitivity analysis is carried out below. Since the depth influence of horizontal loading is 16 m, the deep soil below 16 m is not affected by horizontal loading, and the internal friction angle of deep sand is selected as 32°, which is consistent with the p-y curve method. The elastic constitutive is adopted to describe the pile material, the elastic modulus is 210 GPa, and the Poisson's ratio is 0.3. The calculated parameters of the steel pile foundation and soil are shown in Table 1.

The calculation process of numerical simulation is divided into two steps. Firstly, the initial stress field of the pile and soil is balanced. To realize the initial stress field balance of the pile–soil system, the body force is imposed on the pile–soil system, which is self-weight of the pile–soil system, of which the acceleration of gravity is 1 g. Furthermore, geostatic stresses of soil layers with different depths and K_0 are set separately. After the initial stress field is completely balanced, the horizontal loading is applied on the pile head, and the imposed position of horizontal loading in the numerical simulation is consistent with the field test. To avoid the stress concentration caused by concentrated loading on the pile head, horizontal loading is adopted in the form of surface traction, that is, the horizontal loading is uniformly distributed around the circumference of the pile head, and there are no rigid restraints.

Table 1. Parameters of pile and soil in numerical calculation.

Parameter	E/MPa	ν	c/kPa	φ/°
Steel pile	210,000	0.3	-	-
Mucky silty clay	16.8	0.49	33.6	0.1
Sand	23.75	0.49	1	32

4. Result Analysis and Discussion

Comparison of the horizontal loading–deflection response obtained by the solid finite element method and the p-y curve method and the measured result is illustrated in Figure 8. Since the applied loading in the field-testing pile is relatively small, the initial segment of the loading–deflection response is only compared herein. It can be seen from Figure 8 that calculation results obtained by the solid finite element method are close to measured results in the field test, indicating that the solid finite element method has greater reliability in the foundation design of offshore wind turbines than the p-y curve method under relatively small displacement conditions. With the increase in pile deflection, the difference in calculation results obtained by the solid finite element method and p-y curve method becomes obvious gradually. In detail, when the pile displacement at the mud surface reaches 50 mm, the horizontal loading obtained by the solid finite element method is twice than that from the p-y curve method. Therefore, it needs to be evaluated and analyzed critically whether the solid finite element method or the p-y curve method is selected in the design for offshore wind turbine foundations. In general, the calculation results obtained by the p-y curve method are relatively secure [32,33]. When the pile displacement is relatively small, the calculation result obtained by the solid finite element method is close to the measured result. However, the ratio of the undrained Young's modulus and undrained shear strength (E_u/s_u) is assumed as a constant value in the solid finite element method, that is, the stiffness of the soil is constant, indicating the stiffness of the soil does not decrease with the development of displacement. Therefore, there are some risks of overestimating the bearing capacity of the pile foundation for the solid finite element method under the condition of large displacement.

Figures 9 and 10 are respectively the comparison of bending moment and displacement obtained by the solid finite element method and the p-y curve method and the measured result. Under specific loads (250 kN and 400 kN), no matter the bending moment or displacement of the pile, calculation results obtained by the solid finite element method are relatively small and closer to measured results. However, it can be seen from Figure 9 that when the buried depth exceeds 13 m below the mud surface, the bending moment of the pile obtained by the p-y curve is smaller than that obtained by the solid finite element method, and the overall trend is consistent with measured results. The solid finite element method underestimates the stiffness of the deep soil, thus overestimating the cross-section bending moment of the deep pile. As a result, the partial cross-section design of the pile may be conservative under specific loading conditions (generally small loading), which means that the wall thickness of the pile foundation increases when the pile diameter is constant in the solid finite element method.

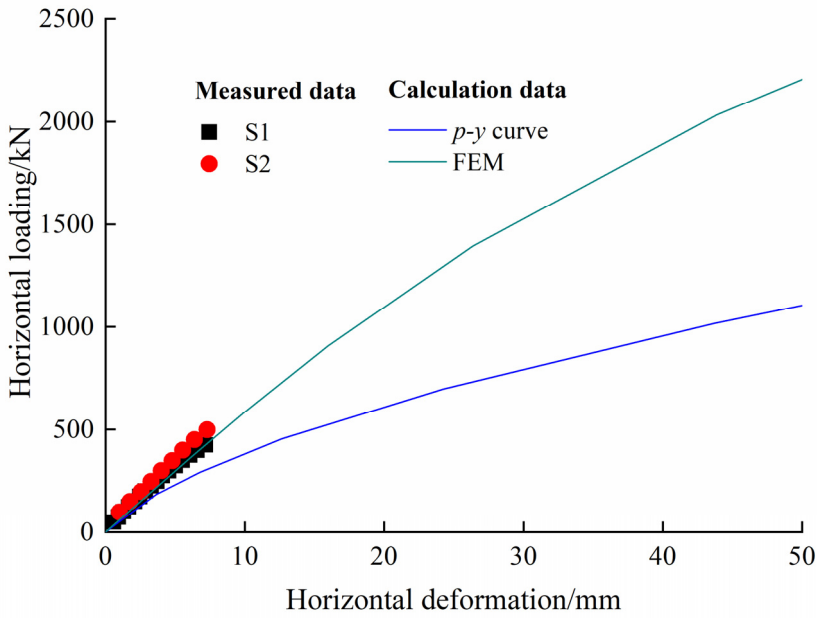

Figure 8. Load–deflection behavior of pile at mud line.

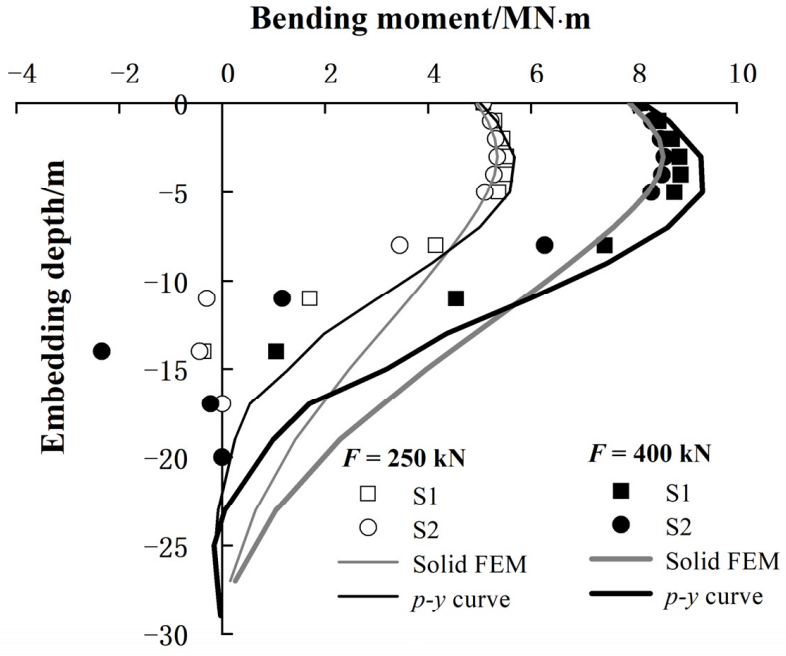

Figure 9. Comparison of pile section moment subjected to 250 kN and 400 kN lateral loads.

The comparison of the p-y curve of the pile–soil system in the shallow layer (up to 4 m below the mud surface) is shown in Figure 11. Under the condition of small displacement, the p-y curve obtained by the solid finite element method is generally close to the p-y curve measured in the field test. It is noted that the p-y curve recommended by the API specification significantly underestimates the initial stiffness of the pile–soil system, and thus overestimates the displacement of the pile under the same loading (Figures 8 and 10). To further compare the difference in formula form of the p-y curves obtained by the solid finite element method and recommended by API, the p-y curves of the soil–pile system at different depths are nondimensionalized, as shown in Figure 12. The p-y curve obtained by the solid finite element method shows a certain degree of gradual degeneration with the increase in buried depth, that is, the relative stiffness of the p-y curve decreases slightly

with the increase in buried depth, therefore, the displacement of the extreme point of the p-y curve increases gradually with the buried depth. The stiffness of the p-y curve recommended by the API specification is significantly less than that from the calculation results of finite element numerical simulation, and the displacement at the extreme point (more than 0.65 *D*) is much larger than that of the solid finite element numerical calculation (about 0.03 *D*). Therefore, the p-y curve recommended by the API specification is generally similar to the flexible pile, resulting in a conservative result (Figure 8). In addition, the form of the p-y curve of the API specification is only related to the strength of the soil, thus the form of the p-y curve obtained by the same or similar soil strength is consistent.

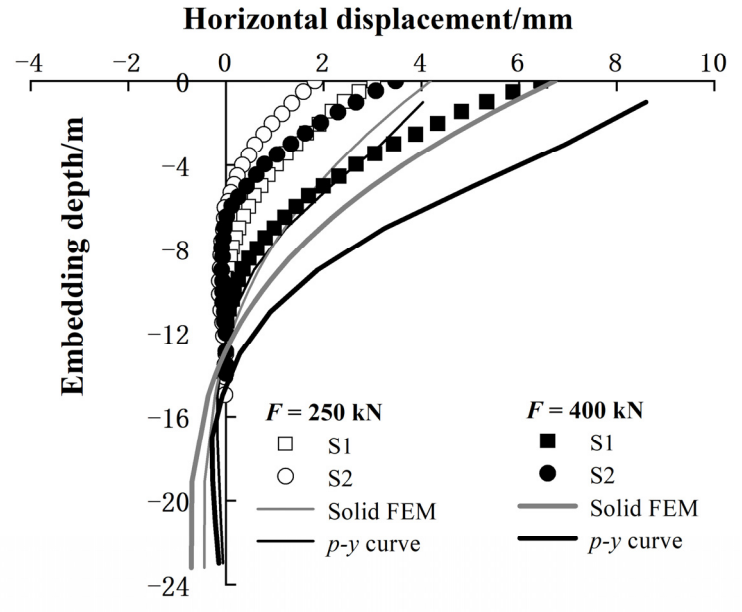

Figure 10. Comparison of pile deflection subjected to 250 kN and 400 kN lateral loads.

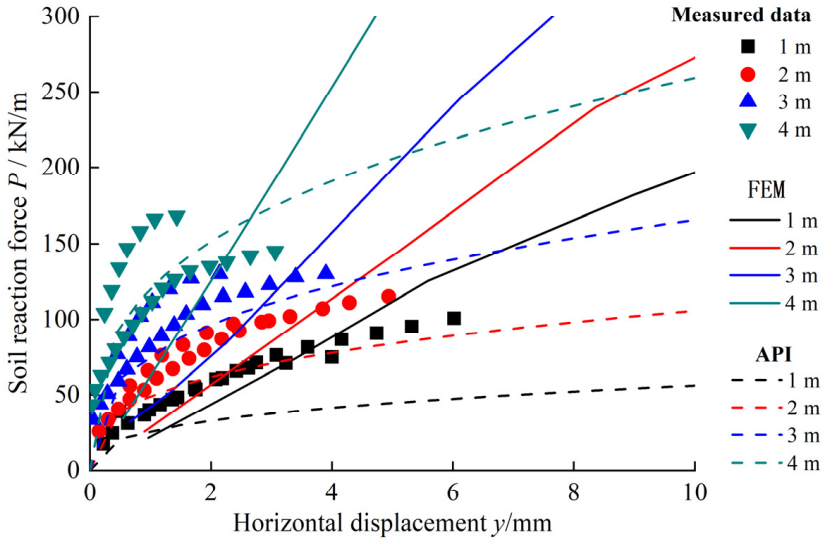

Figure 11. p-y curves by different methods.

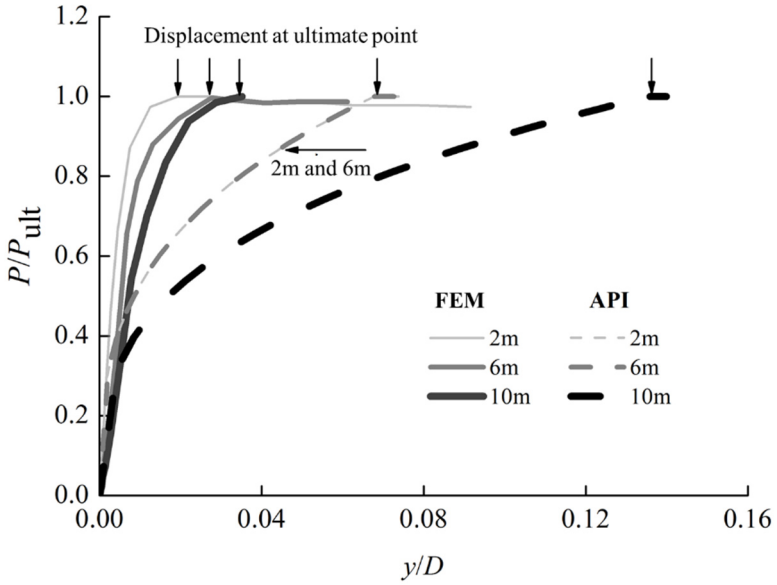

Figure 12. Comparison between p-y curves from solid FEM and API code.

In the establishment of the p-y curve, in addition to determining the basic formula form of the p-y curve, the ultimate soil reaction P_{ult} is also critical. The distribution of the ultimate soil reaction coefficient ($N_p = P_{ult}/s_u D$) of the p-y curve along the buried depth is shown in Figure 13. The soil ultimate reaction calculated by the solid finite element method is the p-y curve of the API specification and is close to the ultimate soil reaction obtained by the p-y curve from the measured field test result. Jeanjean [34] found the ultimate soil reaction coefficient N_p is in the range of 8 to 12 through the centrifugal model test and gradually tends to 12 with the increase in depth. However, according to measured results and calculation results from the solid finite element method, the ultimate soil reaction coefficient N_p of shallow soil is significantly lower than that recommended by Jeanjean [34] and is close to the value recommended by the API specification (3 at mud surface). However, the ultimate soil reaction coefficient calculated by the solid finite element method gradually tends to the value recommended by Jeanjean [34] with the increase in depth, i.e., $N_p = 12$, which is significantly higher than that in the stable state recommended by the API specification ($N_p = 9$). In addition, the ultimate soil reaction is directly related to the failure mode of soil around the pile foundation. For the flexible pile under horizontal loads, soil in front of the pile in the shallow layer has an overall upward deformation and forms the wedge failure zone. The influence range of the horizontal loads at the mud surface is mainly 5.6 m (2D). When the depth exceeds the critical depth, the soil around the pile no longer shows wedge failure and translational movement appears in the same direction as horizontal loads, resulting in the overall flow failure around the pile (or full flow). That is, the failure displacement of the soil layer below the critical depth presents a "flow around the pile" or "full flow" failure zone, that is a wedge failure zone above the critical depth, and the critical depth in the study is 8.5 m (3D), as shown in Figure 14. It can be seen from Figures 13 and 14 that the critical depth of the transition boundary for soil failure mode obtained by the solid finite element method (8.5 m below the mud surface) is slightly smaller than that recommended by the API specification (10 m below the mud surface). Therefore, the increased speed of the ultimate soil reaction calculated by the solid finite element method is fast, and the ultimate soil reaction in a stable state is high, bringing about that the ultimate bearing capacity calculated by the solid finite element method is significantly higher than that obtained by the p-y curve method, as shown in Figure 8.

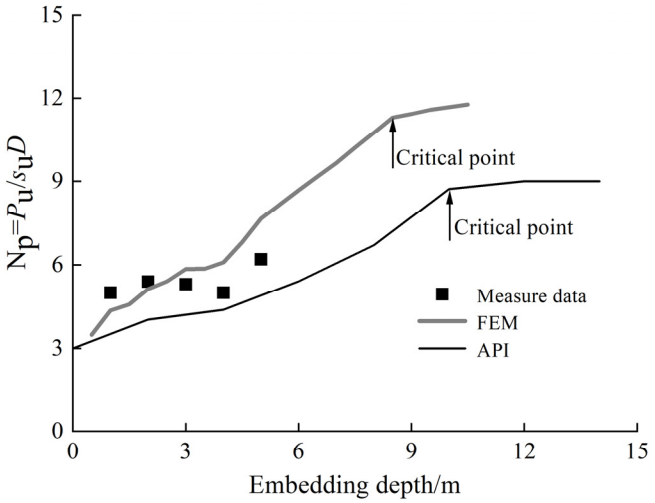

Figure 13. Distribution of N_p values along depth by different methods [35].

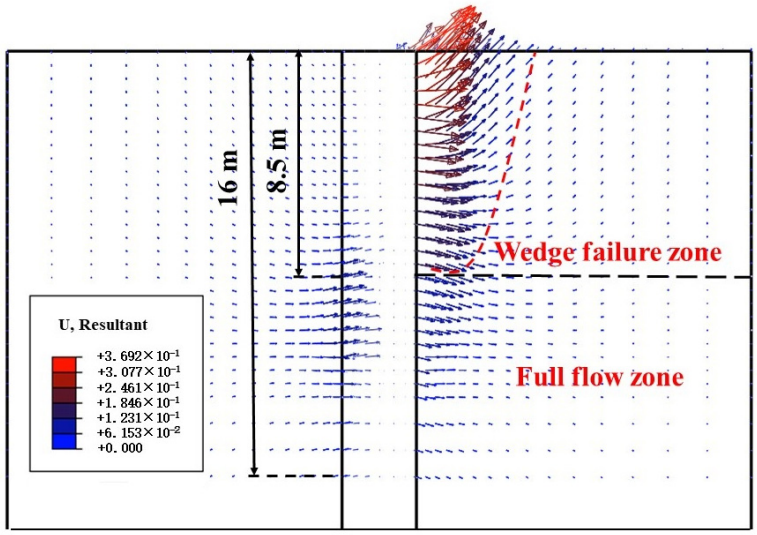

Figure 14. Soil displacement and failure mechanism around pile by solid FEM.

In the design process of pile foundations based on the p-y curve method, it is necessary to establish a specific p-y curve according to API specifications. Therefore, the p-y curve would be completely determined after the calibration of essential property parameters of soil, i.e., the undrained shear strength and internal friction angle, etc., resulting in the divinable and determined horizontal bearing characteristics of pile foundations calculated by the p-y curve. However, there are many relatively uncertain factors for the solid finite element method in the design process of pile foundations, i.e., the modulus ratio of soil, the friction coefficient between the pile and soil, the initial state of soil (K_0), etc., that need to be judged and selected artificially. Therefore, the sensitivity analysis of some key parameters affected by the bearing characteristics is conducted to compare the influence of each parameter on the calculation results of the solid finite element method.

For the flexible pile, especially the steel pipe pile, the ultimate bearing capacity usually corresponds to a larger displacement and rotation angle at the pile head. However, for the specific form of foundation and superstructure of offshore wind turbines, the design characteristics of the structure and the bearing characteristics of the foundation are necessarily considered in the actual design process, and the displacement and rotation angle at the pile head should be limited or stipulated, so as to obtain the ultimate bearing capacity or failure loading [35]. At present, in the design of offshore wind turbine foundations, the displacement of $L/1000$ of the pile on the mud surface is usually used as the control

standard of foundation displacement, where L is the embedded length of the pile into the soil. Therefore, the load corresponding to $L/1000$ (72.5 mm) displacement at the mud surface is adopted as the ultimate bearing capacity of the pile in the study. Figure 15 presents the influence of different influencing factors on the ultimate bearing capacity of piles. It can be seen that the modulus ratio of soil has a great influence on the ultimate bearing capacity of the pile. For soft clay, the upper limit of the ultimate bearing capacity of the pile exceeds 1.7 times the lower limit within a reasonable modulus ratio range (100–800). Moreover, the initial state of soil (K_0) also has a great influence on the bearing characteristics of the pile. When K_0 increases from 0.6 to 1.0, the ultimate bearing capacity of the pile increases by nearly 10%. Since the total stress analysis method is adopted in this study, shallow clay is considered in the undrained state, that is, $K_0 = 1 - sin\varphi$. The internal friction angle (φ) of the undrained clay is taken as 0, therefore, K_0 is valued as 1 for calculation in the study. Relatively speaking, the influence of the friction coefficient of the pile–soil system on the bearing characteristics is relatively small, and the ultimate bearing capacity of piles only differs by 3% based on a friction coefficient within the range (0.2–0.4) recommended by Wang Jincheng and Chen Kaiye [30]. Therefore, the modulus ratio of soil should be carefully selected to obtain accurate calculation results by the solid finite element method. When the solid finite element method is used in the design of the large-diameter monopile foundation of offshore wind turbines without a reliable basis and data, sensitivity and parameter analysis within a reasonable range is suggested to be conducted to select relatively conservative calculation results as the design basis.

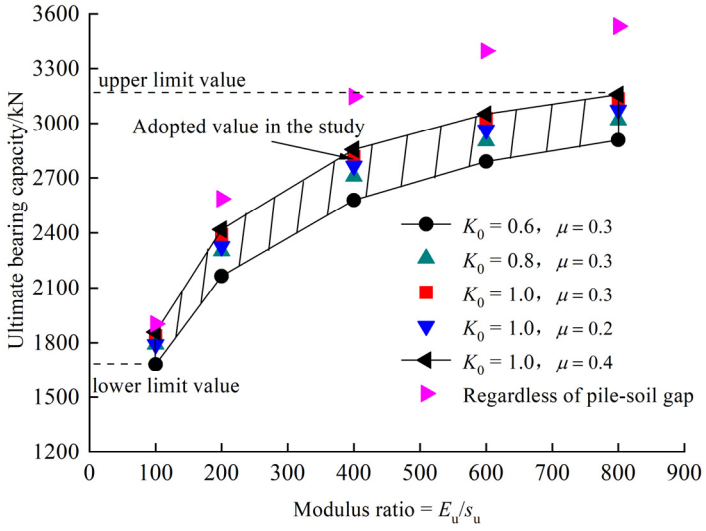

Figure 15. Parameter sensitivity analysis on ultimate capacity of pile.

In addition, it can be seen from Figure 15 that the ultimate bearing capacity of the pile should be significantly increased without considering the detachment effect of the pile–soil system in the solid finite element calculation. Moreover, the greater the soil stiffness, the more significant the detachment effect is on the ultimate bearing capacity; for example, when the modulus ratio is 800, the ultimate bearing capacity of the pile can be increased by 15% without considering the detachment of pile and soil. Because the displacement of $L/1000$ is selected as the determination standard of the ultimate bearing capacity in the study, the influence of pile–soil detachment effect on the bearing capacity of the pile can be more obvious, if the displacement standard is improved. According to Plous and Davies [36], the maximum influence of the pile–soil detachment effect can make the displacement or rotation angle of the pile head increase by 30% to 40%. Therefore, the pile–soil detachment effect must be considered in the design of monopile foundations based on the solid finite element method. Binding the pile and soil will significantly overestimate the stiffness and bearing capacity of the pile foundation, resulting in unsafe design results.

5. Conclusions

Based on the offshore full-scale in situ test result of a pile with the maximum domestic diameter, the study investigated the horizontal loading behavior of monopile foundations by combining two current widely used design methods for an offshore wind turbine, i.e., the p-y curve method and the solid finite element method. Moreover, key technical problems in the design of monopiles are also analyzed and discussed. The main conclusions are summarized below.

(1) The testing pile under horizontal loads presents the typical response of a flexible pile, with the influence range of horizontal loading limited to 5.7 D below the mud surface. The loaded indicator of the testing pile shows a significant linear response with the increase in the loading, i.e., the pile head displacement, bending moment, and deformation of the pile. In addition, the maximum bending moment of the pile gradually moves down with the increase in horizontal loading and tends to be a stable value up to 1.1 D below the mud surface.

(2) There are differences in design results for monopile foundations obtained by the p-y curve and the solid finite element method. The p-y curve recommended by the API specification tends to be flexible on the whole, resulting in a conservative calculation result. Under the condition of small displacement, the calculation result by the solid finite element method is close to the measured result, however, there is a risk of overestimating the ultimate bearing capacity under the condition of large displacement.

(3) The reason for the significant difference between the p-y curve method recommended by the API specification and the solid finite element method is that the stiffness of the p-y curve method recommended by the API specification is significantly lower than that of the finite element method, and its displacement corresponding to the ultimate soil reaction (over 0.65 D) is much larger than that of the solid finite element method (about 0.03 D). Moreover, the stable value of the ultimate reaction (P_{ult}) calculated by the solid finite element method is close to $12s_uD$, which is significantly higher than the recommended value of $9s_uD$ in the API specification.

(4) The design result obtained by the solid finite element method depends heavily on the values of relevant parameters. For an offshore wind farm dominated by clay soil, the upper and lower values of the ultimate bearing capacity of the pile differ by 1.7 times if different modulus ratios are selected. Under the condition that there is no reliable basis, it is suggested that the relatively conservative results obtained by parameter analysis should be used as the design reference in a reasonable range. Without a reliable basis and data, sensitivity and parameter analysis within a reasonable range is suggested to be conducted to select relatively conservative calculation results as the design basis.

(5) The influence of the pile–soil gap must be considered with the solid FEM adopted in the design of the monopile foundation, and bonding between pile and soil can significantly overestimate the stiffness and bearing capacity of the pile, resulting in unsafe design results.

Author Contributions: Formal analysis, T.L. and X.Y.; investigation, T.L., B.H. and S.D.; methodology, T.L. and B.H.; supervision, X.Y. and S.D.; writing—original draft, T.L.; writing—review and editing, X.Y., B.H. and S.D. All authors have read and agreed to the published version of the manuscript.

Funding: The authors appreciate the financial support provided by the National Key Research and Development Program of China (2021YFE0113400), National Natural Science Foundation of China (52171266; 51979155; 52271294), Key Lab Far Shore Wind Power Technol Zhejiang Prov (ZOE2023006).

Institutional Review Board Statement: Not applicable.

Informed Consent Statement: Not applicable.

Data Availability Statement: Data are available upon request.

Conflicts of Interest: Author Tao Li was employed by the company CSSC Haizhuang Windpower Co., Ltd.; Author Ben He was employed by the company Power China Huadong Engineering Corporation Ltd. The remaining authors declare that the research was conducted in the absence of any commercial or financial relationships that could be construed as a potential conflict of interest.

References

1. Wang, X.; Zeng, X.; Li, X.; Li, J. Investigation on offshore wind turbine with an innovative hybrid monopile foundation: An experimental based study. *Renew. Energy* **2019**, *132*, 129–141. [CrossRef]
2. Gupta, B.K.; Basu, D. Offshore wind turbine monopile foundations: Design perspectives. *Ocean Eng.* **2020**, *213*, 107514. [CrossRef]
3. Arany, L.; Bhattacharya, S.; Macdonald, J.; Hogan, S.J. Design of monopiles for offshore wind turbines in 10 steps. *Soil Dyn. Earthq. Eng.* **2017**, *92*, 126–152. [CrossRef]
4. Hu, R.; Lu, Y.; Leng, H.; Liu, H.; Shi, W. A novel countermeasure for preventing scour around monopile foundations using Ionic Soil Stabilizer solidified slurry. *Appl. Ocean Res.* **2022**, *121*, 103121. [CrossRef]
5. Zheng, H.; Du, W.; Li, Y. Development status of offshore wind power at home and abroad. *Hydropower New Energy* **2018**, *32*, 75–77.
6. Zhang, C.; Li, X.; Ma, C.; Li, M. Study on economical efficiency of ocean energy generation in China. *IOP Conf. Ser. Earth Environ. Sci.* **2023**, *1171*, 012003. [CrossRef]
7. Aminoroayaie, Y.O.; Mousavi, S.H.; Kavianpour, M.R.; Movahedi, A. Numerical modeling of sediment scouring phenomenon around the offshore wind turbine pile in marine environment. *Environ. Earth Sci.* **2018**, *77*, 776. [CrossRef]
8. Dai, S.; Han, B.; Wang, B.; Luo, J.; He, B. Influence of soil scour on lateral behavior of large diameter offshore wind turbine monopile and corresponding scour monitoring method. *Ocean Eng.* **2021**, *239*, 109809. [CrossRef]
9. Cuéllar, V.P. *Pile Foundations for Offshore Wind Turbines: Numerical and Experimental Investigations on the Behaviour under Short-Term and Long-Term Cyclic Loading*; Technische Universitaet Berlin: Berlin, Germany, 2011; Volume 257.
10. Alrwashdeh, S.; Al-Saraireh, F.; Alrwashdeh, S.S.; Alsaraireh, F.M. Wind energy production assessment at different sites in Jordan using probability distribution functions. *Artic. ARPN J. Eng. Appl. Sci.* **2018**, *13*, 8163–8172.
11. Alrwashdeh, S.S. Investigation of Wind Energy Production at Different Sites in Jordan Using the Site Effectiveness Method. *Energy Eng. J. Assoc. Energy Eng.* **2019**, *116*, 47–59. [CrossRef]
12. Lau, B.H. *Cyclic Behaviour of Monopile Foundations for Offshore Wind Turbines in Clay*; University of Cambridge: Cambridge, UK, 2015.
13. He, B.; Wang, L.; Hong, Y. Field testing of one-way and two-way cyclic lateral responses of single and jet-grouting reinforced piles in soft clay. *Acta Geotech.* **2017**, *12*, 1021–1103. [CrossRef]
14. Matlock, H. Correlations for design of laterally loaded piles in soft clay. In *Offshore Technology in Civil Engineering's Hall of Fame Papers from the Early Years*; ASCE: Reston, VA, USA, 1970; pp. 77–94.
15. Reese, L.C.; Cox, W.R.; Koop, F.D. Analysis of laterally loaded piles in sand. In *Offshore Technology in Civil Engineering Hall of Fame Papers from the Early Years*; ASCE: Reston, VA, USA, 1974; pp. 95–105.
16. Achmus, M.; Kuo, Y.S.; Abdel-Rahman, K. Behavior of monopile foundations under cyclic lateral load. *Comput. Geotech.* **2009**, *36*, 725–735. [CrossRef]
17. Cheng, X.; Wang, T.; Zhang, J.; Liu, Z.; Cheng, W. Finite element analysis of cyclic lateral responses for large diameter monopiles in clays under different loading patterns. *Comput. Geotech.* **2021**, *134*, 104104. [CrossRef]
18. Kato, B.; Bhattacharya, S.; Wang, Y. Evaluation of post-storm soil stiffness degradation effects on the performance of monopile-supported offshore wind turbines in clay. *Ocean Eng.* **2023**, *282*, 114338. [CrossRef]
19. American Petraleum Institute. Recommended practice for planning, designing and constructing fixed offshore platforms. In *API Recommended Practice 2A-WSD (RP2A-WSD)*, 21st ed.; API: Washington, DC, USA, 2014.
20. Veritas, D.D.N. DNV-OS-J101 Offshore Standard. *Design of Offshore Wind Turbine Structures*. 2010. Available online: https://pdfcoffee.com/dnv-os-j101-design-of-offshore-wind-turbine-structurepdf-pdf-free.html (accessed on 10 November 2023).
21. CCCC Third Harbor Consultants Co., Ltd. *Code for Pile Foundation of Harbor Engineering (JTS167-4-2012)*; China Communications Press: Beijing, China, 2012.
22. Mu, L.; Kang, X.; Li, W. Analytical method for single pile under V-H-M combined loads in sand. *Chin. J. Geotech. Eng.* **2017**, *39*, 153–156. (In Chinese)
23. Lu, W.; Zhang, G. New p-y curve model considering vertical loading for piles of offshore wind turbine in sand. *Ocean Eng.* **2020**, *203*, 107228. [CrossRef]
24. Finn, W.L.; Dowling, J. Modelling effects of pile diameter. *Can. Geotech. J.* **2015**, *53*, 173–178. [CrossRef]
25. Hong, Y.; He, B.; Wang, L. Cyclic lateral response and failure mechanisms of a semi-rigid pile in soft clay: Centrifuge tests and numerical modelling. *Can. Geotech. J.* **2017**, *54*, 806–824. [CrossRef]
26. Lu, F. *Research on the Application of Cone Penetration Test in Offshore Geotechnical Engineering*; Tianjin University: Tianjin, China, 2005.
27. Ministry of Housing and Urban-Rural Development of the People's Republic of China. *Technical Code for Testing of Building Foundation Piles (JGJ 106-2014)*; China Building Industry Press: Beijing, China, 2014.
28. Reese, L.C.; Van Impe, W.F. *Single Piles and Pile Groups under Lateral Loading*; Balkema: Rotterdam, The Netherlands, 2001.

29. Systèmes, D. *Abaqus Analysis User's Manual*; Simulia Corp.: Providence, RI, USA, 2007.
30. Wang, J.; Chen, Y. *Application of ABAQUS in Civil Engineering*; Zhejiang University Press: Hangzhou, China, 2006.
31. Ou, C.; Wu, T.; Hsieh, H. Analysis of Deep Excavation with Column Type of Ground Improvement in Soft Clay. *J. Geotech. Engrg.* **1996**, *122*, 709–716. [CrossRef]
32. Steven, J.B.; Audibert, J.M.E. Re-examination of py curve formulations. In Proceedings of the Offshore Technology Conference, Houston, TX, USA, 30 April–3 May 1979.
33. Zhang, C.; White, D.; Randolph, M. Centrifuge Modeling of the Cyclic Lateral Response of a Rigid Pile in Soft Clay. *Can. Geotech. J.* **2011**, *137*, 717–729. [CrossRef]
34. Jeanjean, P. Re-assessment of p-y curves for soft clays from centrifuge testing and finite element modeling. In Proceedings of the Offshore Technology Conference, Houston, TX, USA, 4–7 May 2009.
35. Chen, Y.; Lee, Y. Evaluation of lateral interpretation criteria for drilled shaft capacity. *J. Geotech. Geoenviron. Eng.* **2010**, *136*, 1124–1136. [CrossRef]
36. Poulos, H.G.; Davis, E.H. *Pile Foundation Analysis and Design*; Wiley: New York, NY, USA, 1980.